DALTON

Towards a model for the oxidized form of purple acid phosphatase: crystal structure and magnetic properties of a binuclear iron(III) complex containing phosphate ligands†

Lihua Yin,[a] Peng Cheng,*[,a] Xinkan Yao[b] and Honggen Wang[b]

[a] *Department of Chemistry, Nankai University, Tianjin 300071, P. R. China*
[b] *Central Laboratory, Nankai University, Tianjin 300071, P. R. China*

A novel binuclear iron(III) complex $[\{FeL[O_2P(OPh)_2]\}_2][ClO_4]_2$ was synthesized and characterized by X-ray single-crystal structure analysis, where HL is bis(benzimidazol-2-ylmethyl)(2-hydroxyethyl)amine. The crystals are triclinic, space group $P\bar{1}$, with $a = 11.523(9)$, $b = 11.809(6)$, $c = 13.406(4)$ Å, $\alpha = 68.52(4)$, $\beta = 71.41(5)$, $\gamma = 71.85(6)°$ and $Z = 1$. The structure shows that the iron(III) ions are bridged by the oxygen atoms of two L ligands and a phosphate ligand is terminally co-ordinated to each iron(III). Magnetic susceptibility measurements in the range 4.2–300 K and subsequent calculations based on an isotropic Heisenberg model suggest antiferromagnetic coupling between the iron(III) ions with $J = -17.5$ cm^{-1}.

The purple acid phosphatases (PAPs) are dinuclear iron enzymes (M 35 000–55 000) which catalyse the *in vitro* hydrolysis of phosphate esters (including nucleoside triphosphates) under acidic pH conditions.[1–4] The purple, inactive forms of uteroferrin and of the phosphatase isolated from bovine spleen contain Fe^{III}–Fe^{III} units in their active sites. The centre of the catalytically active, pink species consists of a Fe^{II}–Fe^{III} core. The oxidized form (purple) can be reduced in a one-electron process to the enzymatically active mixed-valence form (pink). The EPR, Mössbauer and magnetic properties of the two forms indicated that the iron centres are antiferromagnetically coupled in both oxidation states.[5–9] The PAPs thus belong to a class of diiron proteins[2] which includes haemerythrin,[10,11] methane monooxygenase[12,13] and the R2 protein of ribonucleotide reductase.[14] In this class of diiron proteins, suitable crystals of PAPs have yet to be obtained for X-ray crystallographic examination. Based on the spectroscopic, magnetic and EXAFS (extended X-ray absorption fine structure) investigations, the proposed structure of the active form of PAP from bovine spleen exhibits a terminally co-ordinated phosphate ligand[6,15,16] or phosphate bridging ligand.[17] Very recently, Krebs and co-workers[18,19] reported the crystal structure of kidney bean purple acid phosphatase at 2.9 Å resolution. It contains one zinc(II) ion and one iron(III) ion and has a similar site to that in the mammalian Fe^{II}–Fe^{III} purple acid phosphatase. The zinc(II) and iron(III) ions are 3.1 Å apart and bridged monodentately by the Asp-164 residue. The iron is further co-ordinated by the Tyr-167, His-325 and Asp-135, and the zinc by the His-286, His-323 and Asn-201 residues. The active-site structure supports a mechanism of phosphate ester hydrolysis involving nucleophilic attack on the phosphate group by an Fe^{III}-co-ordinated hydroxide ion. Diiron-(II,III) and -(III,III) model compounds containing a bridging co-ordination of phosphate and phosphate ester have been synthesized and characterized in some cases.[20–27] The diiron complexes with terminally co-ordinated phosphate ligands, however, are poorly understood.[28]

In this paper we report a novel binuclear iron(III) complex with terminally co-ordinated phosphate ligands, using the polydentate ligand bis(benzimidazol-2-ylmethyl)(2-hydroxyethyl)-amine.

† *Non-SI unit employed:* $\mu_B \approx 9.27 \times 10^{-24}$ J T^{-1}.

Experimental

Bis(benzimidazol-2-ylmethyl)(2-hydroxyethyl)amine (HL) was synthesized by published procedures.[29] All other chemicals used in this work were reagent grade and used as commercially obtained.

Preparations

Reaction of a 1 : 1 : 1 molar ratio (0.5 mmol) of bis(benzimidazol-2-ylmethyl)(2-hydroxyethyl)amine, $Fe(ClO_4)_3 \cdot 9H_2O$ and diphenyl phosphate in methanol (30 cm^3) for 30 min afforded red microcrystals of $[\{FeL[O_2P(OPh)_2]\}_2][ClO_4]_2$ (yield 80%) (Found: C, 49.1; H, 4.25; N, 10.15; P, 3.95. $C_{60}H_{56}Cl_2Fe_2N_{10}O_{18}P_2$ requires C, 49.65; H, 3.85; N, 9.65; P, 4.25%). Red crystals suitable for X-ray single-crystal structure analysis were obtained by diffusion.

Physical measurements

The analyses (C, H, N, P) were performed at MHW laboratories (Phoenix, AZ, USA). The ^{1}H NMR spectrum was recorded on an IBM AC300 spectrometer at 300 MHz and the chemical shifts (in ppm) were referenced to the residual protic solvent peak, the infrared spectrum on Perkin-Elmer 1800FT-IR spectrometer by using KBr pellets and electronic spectra (MeOH) on a Hitachi model 240 spectrometer at room temperature. Variable-temperature magnetic susceptibilities were measured on a vibrating-sample magnetometer, model CF-1, in the temperature range 4.2–300 K. Diamagnetic corrections were made with Pascal's constants for all the substituent atoms,[30] and the magnetic moments were calculated using the equation $\mu_{eff} = 2.828(\chi T)^{\frac{1}{2}}$. The theoretical expression was fitted to the data by applying a least-squares refinement.

X-Ray crystallography

Details of crystal parameters, data collection and structure refinement are summarized in Table 1. The structure was solved by the direct methods (MULTAN 82).[31] The iron atom positions were located in the initial E maps. The other non-hydrogen atoms were determined with successive Fourier-difference syntheses. Hydrogen atoms were not found. The final refinement (based on F) was by full-matrix least squares with unweighted and weighted agreement R factors of 0.058 and 0.063. The highest peak on the final Fourier-difference map had

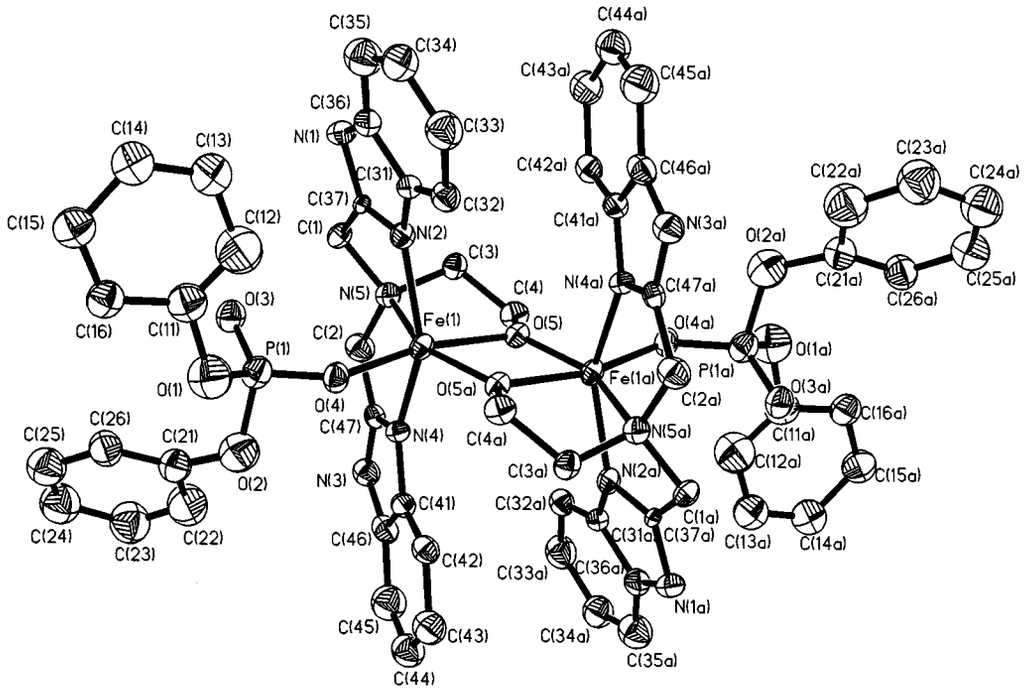

Fig. 1 An ORTEP view of the complex with the atom numbering scheme

the value of 0.44 e A^{-3}. All calculations were performed on PDP 11/44 and IBM 586 computers using the ORTEP program system[33] for molecular graphics.

Atomic coordinates, thermal parameters, and bond lengths and angles have been deposited at the Cambridge Crystallographic Data Centre (CCDC). See Instructions for Authors, *J. Chem. Soc., Dalton Trans.*, 1997, Issue 1. Any request to the CCDC for this material should quote the full literature citation and the reference number 186/487.

Results and Discussion

Spectral characterization

The IR spectrum of the complex showed ν(P=O) at 1202 cm^{-1} and ν(P–O–Ph) at 929 cm^{-1}, respectively. The strong absorption at 1100–1120 cm^{-1} may be overlap of ν(ClO_4) and ν(P–O). The ν(NH) and ν(C=N) bands of benzimidazole are observed at 3450 and 1490 cm^{-1}. The bands at 745 and 532 cm^{-1} should be assigned to ν_{asym}(Fe–O–Fe) and ν_{sym}(Fe–O–Fe), respectively. The ^{1}H NMR spectrum of the complex measured in Me_2SO solution exhibits paramagnetically shifted features. The sharp features at δ 7.7 and 8.0 correspond to the protons of the benzene ring of diphenyl phosphate. The broad peaks at δ 42.2 and 60.0 should be assigned to the protons of C(32)H and N(1)H of benzimidazole, which indicate that the N(2) nitrogen atoms are co-ordinated to iron(III) ions. The electronic spectrum of the complex in methanol shows absorption maxima at λ_{max} = 214, 245, 270 and 451 nm (sh). An absorption maximum in the region of the charge-transfer transition of PAP (500–600 nm) could not be observed for the complex owing to the absence of phenolate oxygen donors.[28]

Crystal structure

The complex $[\{FeL[O_2P(OPh)_2]\}_2][ClO_4]_2$ crystallizes in the triclinic space group *P*1. The structure of the cation of the complex and a stereoview of the unit cell are shown in Figs. 1 and 2, respectively. Selected bond lengths and angles are given in Table 2. The iron atoms in the centrosymmetric, binuclear structure are bridged by the oxygen atoms of the two L ligands. Each of these L ligands also binds one Fe atom through three nitrogen atoms (the tertiary N atom and one from each benzimidazole group) in a meridional mode. The very distorted octahedral co-

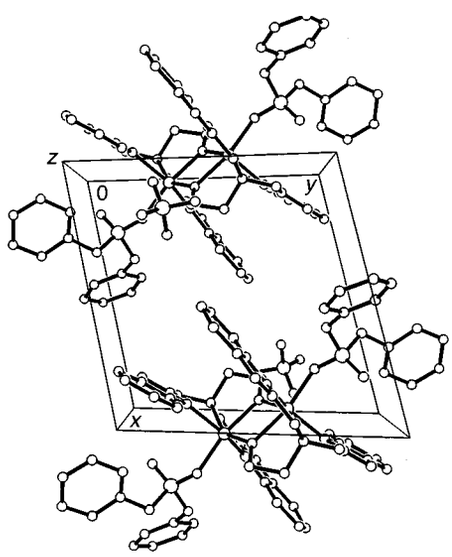

Fig. 2 Stereoview of the unit cell

ordination about the Fe atom is completed by the terminal binding of a phosphate ligand. The Fe···Fe distance is 3.165 Å, which is very similar to that in kidney bean PAP (3.1 Å),[18] and bovine spleen enzyme (3.00 Å)[15] and uteroferrin (3.15 or 3.52 Å)[17] based on EXAFS studies. The complex exhibits a Fe···P distance of 3.137 Å, which is about 0.21 Å shorter than that found in $[Fe_2Cl_2\{O_2P(OPh)_2\}(tbpo)(MeOH)][ClO_4]_2\cdot 3MeOH$ [Htbpo = *N*,*N*,*N*′,*N*′-tetrakis(benzimidazol-2-ylmethyl)-2-hydroxypropane-1,3-diamine] in which a phosphate ligand is terminally co-ordinated to iron(III) ion.[28] This distance is also shorter than that in phosphate-bridged diiron(III) complexes and near to that in PAP from beef spleen (3.06 Å)[16] and uteroferrin (3.17 Å).[17]

Magnetic properties

The variable-temperature susceptibility of the complex has been recorded in the region 4.2–300 K. The magnetic moment (μ_{eff}) at room temperature is 6.22 μ_B. With lowering of the temperature, the magnetic moment of the complex decreases and reaches 0.64 μ_B at 8.7 K. This magnetic behaviour suggested that the operation of an antiferromagnetic spin exchange

Table 1 Crystallographic data and data-collection parameters for the complex

Formula	$C_{60}H_{56}Cl_2Fe_2N_{10}O_{18}P_2$
M	1449.72
Crystal system	Triclinic
Space group	$P\bar{1}$
a/Å	11.523(9)
b/Å	11.809(6)
c/Å	13.406(4)
α/°	68.52(4)
β/°	71.41(5)
γ/°	71.85(6)
U/Å^3	1569(2)
Z	1
D_c/g cm^{-3}	1.53
Crystal dimensions/mm	0.1 × 0.2 × 0.3
Colour	Purple
T/K	299 ± 1
Radiation (λ/Å)	Mo-Kα (0.710 73)
Monochromator	Graphite
μ/mm^{-1}	0.675
Absorption correction applied	Empirical[a]
Transmission factors: min., max.	0.730, 1.192
Diffractometer	Enraf-Nonius CAD4
Scan method	ω–2θ
h, k, l Limits	−12 to 12, −13 to 13, 0–14
θ_{max}/°	23
Scan speed/° min^{-1}	0.92–5.49
Programs used	Enraf-Nonius SDP-PLUS[b]
F(000)	746
w	1 for all observed reflections
Data collected	4512
Unique data	4082
Data with $I \geqslant 3\sigma(I)$	1168
R_{int}	0.207
No. variables	424
Largest shift/e.s.d. in final cycle	0.51
R[c]	0.058
R'[d]	0.063

[a] See ref. 32. [b] See ref. 31. [c] $R = \Sigma||F_o| - |F_c||/\Sigma|F_o|$. [d] $R' = [\Sigma w(|F_o| - |F_c|)^2/\Sigma w|F_o|^2]^{\frac{1}{2}}$; $w = 1/\sigma^2(F_o)$.

Table 2 Selected bond distances (Å) and angles (°)

Fe(1) · · · Fe(1a)	3.165	Fe(1) · · · P(1)	3.137
Fe(1)–O(4)	1.999(8)	Fe(1)–O(5a)	1.910(7)
Fe(1)–O(5)	2.055(8)	Fe(1)–N(2)	2.10(1)
Fe(1)–N(4)	2.076(9)	Fe(1)–N(5)	2.34(1)
P(1)–O(1)	1.58(1)	P(1)–O(2)	1.63(2)
P(1)–O(3)	1.415(8)	P(1)–O(4)	1.426(9)
O(4)–Fe(1)–O(5a)	93.8(3)	O(4)–Fe(1)–O(5)	167.1(3)
O(4)–Fe(1)–N(2)	89.8(3)	O(4)–Fe(1)–N(4)	88.8(3)
O(4)–Fe(1)–N(5)	114.4(4)	O(5a)–Fe(1)–O(5)	74.1(4)
O(5a)–Fe(1)–N(2)	109.6(4)	O(5a)–Fe(1)–N(4)	104.7(4)
O(5a)–Fe(1)–N(5)	151.7(3)	O(5)–Fe(1)–N(2)	98.2(3)
O(5)–Fe(1)–N(4)	90.2(3)	O(5)–Fe(1)–N(5)	77.6(3)
N(2)–Fe(1)–N(4)	145.8(4)	N(2)–Fe(1)–N(5)	74.7(4)
N(4)–Fe(1)–N(5)	74.9(4)	O(1)–P(1)–O(2)	98.5(6)
O(1)–P(1)–O(3)	114.4(6)	O(1)–P(1)–O(4)	109.1(5)
O(2)–P(1)–O(3)	108.8(6)	O(2)–P(1)–O(4)	105.8(6)
O(3)–P(1)–O(4)	118.2(5)	Fe(1)–O(5a)–Fe(1a)	105.9(4)
Fe(1)–O(4)–P(1)	131.9(5)	Fe(1)–O(5a)–C(4a)	134.3(6)
Fe(1)–O(5a)–C(4)	118.7(6)	Fe(1)–N(2)–C(31)	133.9(8)
Fe(1)–N(2)–C(37)	115.7(8)	Fe(1)–N(4)–C(41)	129.9(9)
Fe(1)–N(4)–C(47)	119.5(9)	Fe(1)–N(5)–C(1)	108.1(6)
Fe(1)–N(5)–C(2)	111.2(7)	Fe(1)–N(5)–C(3)	103.5(7)

Symmetry transformation: a $-x$, $1-y$, $1-z$.

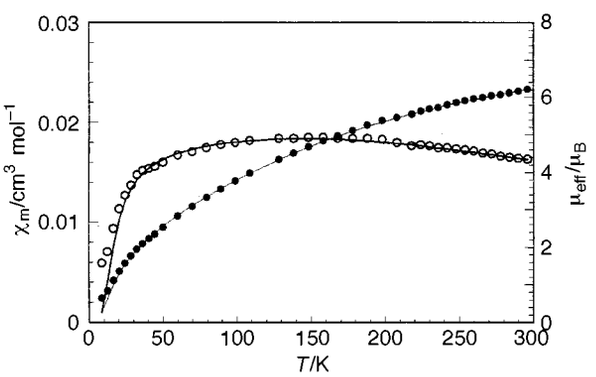

Fig. 3 The experimental data and fitted curves of magnetic susceptibilities (○) and moments (●) of the complex

occurs in the complex. The magnetic data could be fitted on the basis of an isotropic Heisenberg model $H = -2JS_1S_2$ ($S_1 = S_2 = \frac{5}{2}$) [equation (1)], where $A = 55 + 30\exp(-10J/kT) +$

$$\chi_m = \frac{2Ng^2\beta^2}{kT}\,\frac{A}{B} \qquad (1)$$

$14\exp(-18J/kT) + 5\exp(-24J/kT) + \exp(-28J/kT)$, $B = 11 + 9\exp(-10J/kT) + 7\exp(-18J/kT) + 5\exp(-24J/kT) + 3\exp(-28J/kT) + \exp(-30J/kT)$, χ_m is the molecular susceptibility and the other symbols have their usual meanings. The experimental data and fitted curves of magnetic susceptibilities and moments are shown in Fig. 3. The parameters found were $J = -17.5$ cm^{-1} and $g = 2.01$. The agreement factor R, defined as $\Sigma[(\chi_m^{obs} - \chi_m^{calc})^2/(\chi_m^{obs})^2]$, is 3.5×10^{-3}. The value of the exchange integral (-17.5 cm^{-1}) is expected to fall in the range of μ-alkoxo- or μ-hydroxo-bridged binuclear iron(III) systems and slightly larger (absolute value) than the complex with a terminally co-ordinated phosphate ligand (-13.7 cm^{-1}).[28]

The binuclear iron(III) complex, with a bis(alkoxo) bridge and the terminal monodentate phosphate ester ligands, is expected to be weakly antiferromagnetically coupled. This structural feature is actually of more interest regarding the co-ordination mode of the substrate to the reduced ($Fe^{II}Fe^{III}$) core of the enzyme, where monodentate ligation [to the iron(II) ion] seems likely, rather than to the oxidized (Fe^{III}_2) form of the enzyme, for which most evidence favours a bidentate bridging co-ordination mode. The magnetic susceptibility results suggest that the amount of coupling may be an order of magnitude larger than that in magnetically coupled high-spin $Fe^{II}Fe^{III}$ centres,[6,8] but in agreement with the recent magnetic susceptibility studies on oxidized PAP from bovine spleen.[34] Similarly, the bis(alkoxo) bridging is a reasonable model for the monodentate bridging carboxylate/bridging hydroxide unit that is probably present in the enzyme.

Acknowledgements

This work was supported by the National Natural Science Foundation of China.

References

1 K. Doi, B. C. Antanaitis and P. Aisen, *Struct. Bonding* (*Berlin*), 1988, **70**, 1.
2 L. Que, jun. and A. E. True, *Prog. Inorg. Chem.*, 1990, **38**, 97.
3 J. B. Vincent and B. A. Averill, *FASEB J.*, 1990, **4**, 3009.
4 R. G. Wilkin, *Chem. Soc. Rev.*, 1992, **21**, 171.
5 B. C. Antanaitis, P. Aisen and H. R. Lilienthal, *J. Biol. Chem.*, 1983, **258**, 3166.
6 B. A. Averill, J. C. Davis, S. Burman, T. Zirino, J. Sanders-Loehr, T. M. Loehr, J. T. Sage and P. G. Debrunner, *J. Am. Chem. Soc.*, 1987, **109**, 3760.
7 P. G. Debrunner, M. P. Hendrich, J. de Jersey, D. T. Keough, J. T. Sage and B. Zenner, *Biochim. Biophys. Acta*, 1983, **745**, 103.
8 E. P. Day, S. S. Davis, J. Peterson, W. R. Dunham, J. J. Bonvoisin, R. H. Sands and L. Que, jun., *J. Biol. Chem.*, 1988, **263**, 15 561.
9 E. Sinn, C. J. O'Connor, J. de Jersey and B. Zerner, *Inorg. Chim. Acta*, 1983, **78**, L13.

10 R. E. Stenkamp, L. C. Sieker and L. H. Jensen, *J. Am. Chem. Soc.*, 1984, **106**, 618.
11 S. Sheriff, W. A. Hendrickson and J. L. Smith, *J. Mol. Biol.*, 1987, **197**, 273.
12 B. G. Fox, W. A. Forland, J. E. Dege and J. D. Lipscomb, *J. Biol. Chem.*, 1989, **264**, 10 023.
13 A. C. Rosenzweig, C. A. Frederick, S. J. Lippard and P. Nordlund, *Nature* (*London*), 1993, **366**, 537.
14 P. Nordlund, B.-M. Sjoberg and H. Eklund, *Nature* (*London*), 1990, **345**, 593.
15 S. M. Kauzlarich, B. K. Teo, T. Zirino, S. Burman, J. C. Davis and B. A. Averill, *Inorg. Chem.*, 1986, **25**, 2781.
16 R. C. Scarrow, J. W. Pyrz and L. Que, jun., *J. Am. Chem. Soc.*, 1990, **112**, 657.
17 A. E. True, R. C. Scarrow, C. R. Randall, R. C. Holz and L. Que, jun., *J. Am. Chem. Soc.*, 1993, **115**, 4246.
18 N. Strater, T. Klabunde, P. Tucker, H. Witzel and B. Krebs, *Science*, 1995, **268**, 1489.
19 T. Klabunde, N. Strater, R. Frohlich, H. Witzel and B. Krebs, *J. Mol. Biol.*, 1996, **259**, 737.
20 K. Schepers, B. Bremer, B. Krebs, G. Henkel, E. Althaus, B. Mosel and W. Muller-Warmuth, *Angew. Chem., Int. Ed. Engl.*, 1990, **29**, 531.
21 B. Krebs, K. Schepers, B. Bremer, G. Henkel, E. Althaus, B. Mosel, W. Muller-Warmuth, K. Griesar and W. Hasse, *Inorg. Chem.*, 1994, **33**, 1907.
22 S. Drueke, K. Wieghardt, B. Nuber, J. Weiss, H. P. Fleischhauer, S. Gehring and W. Hasse, *J. Am. Chem. Soc.*, 1989, **111**, 8622.
23 W. H. Armstrong and S. J. Lippard, *J. Am. Chem. Soc.*, 1985, **107**, 3730.
24 P. N. Turowski, W. H. Armstrong, M. E. Roth and S. J. Lippard, *J. Am. Chem. Soc.*, 1990, **112**, 681.
25 S. Yan, D. D. Cox, L. L. Pearce, C. Juarez-Garcia, L. Que, jun., J. H. Zhang and C. J. O'Connor, *Inorg. Chem.*, 1989, **28**, 2507.
26 R. E. Norman, S. Yan, L. Que, jun., G. Backes, J. Ling, J. Sanders-Loehr, J. H. Zhang and C. J. O'Connor, *J. Am. Chem. Soc.*, 1990, **112**, 1554.
27 P. N. Turowski, W. H. Armstrong, S. Liu, S. N. Brown and S. J. Lippard, *Inorg. Chem.*, 1994, **33**, 636.
28 B. Bremer, K. Schepers, P. Fleischhauer, W. Haase, G. Henkel and B. Krebs, *J. Chem. Soc., Chem. Commun.*, 1991, 510.
29 Y. Nishida and K. Takahashi, *J. Chem. Soc., Dalton Trans.*, 1988, 691.
30 E. A. Boudreaux and L. N. Mulay, *Theory and Application of Molecular Paramagnetism*, Wiley, New York, 1976, p. 491.
31 SDP-PLUS, B. A. Frenz & Associates, Inc., College Station, TX and Enraf-Nonius, Delft, 1985.
32 N. Walker and D. Stuart, *Acta Crystallogr., Sect. A*, 1983, **39**, 158.
33 C. K. Johnson, ORTEP, a Fortran thermal-ellipsoid plot program for crystal structure illustrations, Report ORNL-5138 (third revision), Oak Ridge Natonal Laboratory, Oak Ridge, TN, 1976.
34 S. Gehring, P. Fleischhauer, W. Haase, M. Dietrich and H. Witzell, *Biol. Chem. Hoppe-Seyler*, 1990, **371**, 786.

Received 10*th December* 1996; *Paper* 6/08298J